ChemComm

COMMUNICATION

View Article Online
View Journal | View Issue

Cite this: *Chem. Commun.*, 2017, 53, 9554

Received 16th June 2017,
Accepted 2nd August 2017

DOI: 10.1039/c7cc04701k

rsc.li/chemcomm

Ti_2Au_2C and $Ti_3Au_2C_2$ formed by solid state reaction of gold with Ti_2AlC and Ti_3AlC_2†

H. Fashandi, C.-C. Lai, M. Dahlqvist, J. Lu, J. Rosen, L. Hultman, G. Greczynski, M. Andersson, A. Lloyd Spetz and P. Eklund *

Incorporation of layers of noble metals in non-van der Waals layered materials may be used to form novel layered compounds. Recently, we demonstrated a high-temperature-induced exchange process of Au with Si in the layered phase Ti_3SiC_2, resulting in the formation of Ti_3AuC_2 and $Ti_3Au_2C_2$. Here, we generalize this technique showing that Au/Ti_2AlC and Au/Ti_3AlC_2 undergo an exchange reaction at 650 °C to form Ti_2Au_2C and $Ti_3Au_2C_2$ and determine their structures by electron microscopy, X-ray diffraction, and *ab initio* calculations. These results imply that noble-metal-containing layered phases should be possible to synthesize in many systems. The metal to be introduced should be inert to the transition-metal carbide layers, and exhibit negative heat of mixing with the initial A element in a liquid phase or two-phase liquid/solid region at the annealing temperature.

Phases with nanolaminated or atomically layered structures are an extensive research topic for the synthesis of novel materials and two-dimensional structures. Layered ceramics constitute a large class of materials including both van der Waals (vdW) materials, such as graphite or transition-metal dichalcogenides, and non-vdW solids. vdW materials are commonly applied for the formation of new two-dimensional materials, and allow for intercalation of foreign species, both ionic such as in Li-ion batteries[1,2] and neutral as in the case of intercalation of zerovalent noble metals in vdW solids.[3–5] In contrast, incorporation of noble-metal layers in non-vdW layered materials to form novel compounds is an outstanding challenge.

Recently, we demonstrated a high-temperature-induced exchange process of Au with Si in the layered phase Ti_3SiC_2, resulting in the formation of the novel Ti_3AuC_2 and $Ti_3Au_2C_2$ phases by an ordered replacement of the A-layer crystal planes; from Si-planes to Au or Au_2 planes.[6] Furthermore, Ir-exchange with Au in Ti_3AuC_2 yielded the new phase Ti_3IrC_2.[6] The starting phase Ti_3SiC_2 is an archetype member of the $M_{n+1}AX_n$ phases, a large family of layered transition-metal carbides and nitrides[7–10] that exhibits an unusual combination of metallic and ceramic properties. In this notation, M is an early transition metal, A is normally an element from groups 12–16, X is carbon or nitrogen, and n is typically 1–3. These phases can also be exfoliated to form a recently established class of two-dimensional materials labelled MXene.[11–16] The introduction of Au in $M_{n+1}AX_n$ phases by high-temperature-induced exchange can be used for Ga-containing MAX phases (Mo_2GaC and Mo_2Ga_2C[17,18]) to synthesize Mo_2AuC and $Mo_2(Au_{1-x}Ga_x)_2$ through an Au substitution reaction with Ga.[19]

The question remains whether this mechanism can be generally applied to other $M_{n+1}AX_n$ phases, and beyond. We chose thin films of Ti_2AlC and Ti_3AlC_2 as model system to address this question. Unlike the only two known $M_{n+1}(Si)X_n$ phases (Ti_3SiC_2 and Ti_4SiC_3), there are more than a dozen different $M_{n+1}(Al)X_n$ phases.[7,8] Demonstration of an Au-exchange reaction here would strongly indicate the generality of the process and help formulating general guiding principles.

Annealing of Au-capped Ti_2AlC thin films on *c*-plane sapphire samples was performed at 650 °C in nitrogen atmosphere for 10 h. After the annealing, we studied the surface of the samples using SEM to find any traces of out-diffused species from underneath the Au layer. As previously reported,[6] Si was observed to out-diffuse to the surface of Au/Ti_3SiC_2/SiC samples due to Au-exchange reaction within Ti_3SiC_2. Fig. 1 shows the SEM/EDX analysis of the annealed samples. Prior to the annealing, the surface of the as-deposited Au capping layer on Ti_2AlC was uniform. After the annealing, some clusters appeared on the surface (see Fig. 1(a)). Fig. 1(b) illustrates one of these clusters. Using EDX, we mapped the Ti-Kα signal of Fig. 1(b) to identify the clusters. As can be seen in Fig. 1(c), a weak and uniform mapping for Ti-Kα was acquired showing the cluster to be deficient in Ti, as the rest of the Au surface. This excludes that the observed clusters could be due to exposure of the Ti_2AlC sublayer. Fig. 1(d) and (e) show the EDX mappings of Au-Mα and Al-Kα signals of Fig. 1(b), respectively. Fig. 1(d) shows the Au layer surrounding the cluster, the latter not containing any Au. Fig. 1(e)

Department of Physics, Chemistry, and Biology (IFM), Linköping University, SE-581 83 Linköping, Sweden. E-mail: per.eklund@liu.se

† Electronic supplementary information (ESI) available: Materials and methods, additional characterization, density functional theory results. See DOI: 10.1039/c7cc04701k

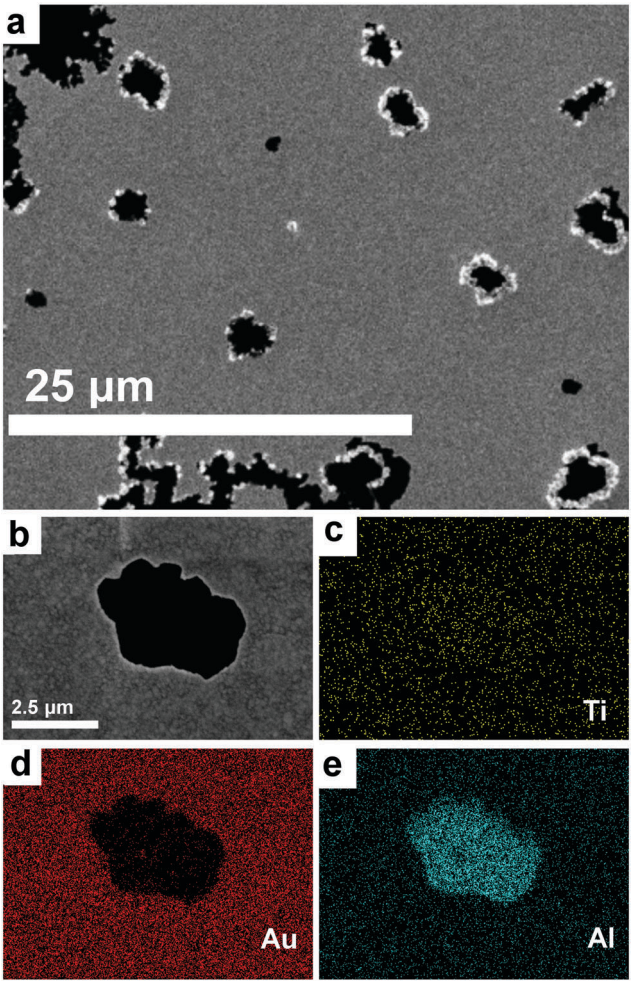

Fig. 1 SEM of the surface of annealed Au/Ti_2AlC. (a) Low-magnification overview image of the surface. (b) Magnified image of a single feature. (c–e) EDX mapping of Ti-Kα, Au-Mα, and Al-Kα signals of (b), respectively.

reveals the spot to be primarily composed of Al. The clusters are not observed in XRD (below) and thus most likely amorphous aluminum with oxygen from the ambient. The same features were also observed for the case of Au/Ti_3AlC_2/sapphire samples, confirming that Al had diffused out of the Ti_2AlC and Ti_3AlC_2 layers during the annealing procedure (see ESI†). This observation is consistent with an exchange reaction, but alone is not sufficient proof of such a reaction, since out-diffusion of the A-element from $M_{n+1}AX_n$ phases is an expected feature in case of high-temperature decomposition and/or oxidation.[20–22]

We used scanning transmission electron microscopy (STEM) to study how Al out-diffusion affects the crystal structure of Ti_2AlC and Ti_3AlC_2. Fig. 2(a) is an overview STEM image of an annealed Au/Ti_2AlC/sapphire sample. In STEM, the brightness is directly proportional to the mass. As can be seen, the phase has a layered structure as expected from $M_{n+1}AX_n$ phases. The common pattern of the structure is comprised of alternating layers of heavy (Au) and light (Ti) elements with approximately the same thicknesses. Fig. 2(b), which is a higher magnification STEM/EDX of Fig. 2(a), shows that the heavy layers are Au-double-layers instead of Al-monolayers as in the initial Ti_2AlC. This result confirms the exchange reaction of Au into Ti_2AlC. The reaction occurs by Au in-diffusion along domain boundaries and basal planes, with Al diffusing in the opposite direction (*cf.*, Au and Si in ref. 6). Based on the EDX results, the Al content of the Au sites is negligible and thus we refer to it as Ti_2Au_2C.

Fig. 2(c) shows the crystal structure of Ti_2Au_2C viewed with the electron beam along two different orientations, $[11\bar{2}0]$ and $[1\bar{1}00]$. The Ti_2C sheets possess a zig-zag pattern with respect to each other, while Au_2 layers have the same inclination, *i.e.*, a zig-zig pattern relative to one another. This can be obtained within two different unit cells within two different space groups, $P\bar{3}m1$ and $P\bar{3}m1$ (see ESI†). Density functional theory (DFT) *ab initio* calculations were used to determine the possible crystal structures for Ti_2Au_2C (see ESI†). According to these theoretical results, the crystal described within the $P\bar{3}m1$ symmetry has lower energy. Furthermore, the corresponding lattice shows dynamical stability based on the all-positive frequencies in the simulated phonon dispersion plots. Thus, we conclude that the description within the $P\bar{3}m1$ space group matches the crystal structure of Ti_2Au_2C (see ESI† the corresponding unit cell and for individual atom positions). XPS analysis (see ESI†) indicates a degree of negative charge transfer from Au to Ti atoms.

A STEM/EDX study on Au/Ti_3AlC_2/sapphire samples also showed the replacement of the Al-monolayers with Au double-layers (see Fig. 2(d) for an overview image). This is confirmed by the STEM/EDX mapping illustrated in Fig. 2(e). Like for Ti_2Au_2C, EDX showed negligible Al content in the Au sites. These results demonstrate formation of the phase $Ti_3Au_2C_2$. Fig. 2(f) shows the atomic positions with the beam along two different orientations, $[11\bar{2}0]$ and $[1\bar{1}00]$. Ti_3C_2 sheets have a zig-zag pattern along $[11\bar{2}0]$. Double-layers of Au are formed with the two monolayers placed in a closed-packed configuration on top of each other. This is different from Mo_2Ga_2C, in which Ga atoms forming the corresponding Ga double-layers reside on top of each other normal to the layers.[17,18] In Ti_3SiC_2, the insertion of monolayers of Au resulted in the growth of Ti_3AuC_2, insertion of Au-double layers was also achieved. The Au_2 layers acquired a general zig-zig–zag-zag pattern with respect to each other. It should be noted that there are numerous stacking faults in the present samples. The structure of $Ti_3Au_2C_2$ is the same as that in ref. 6 in the $P\bar{3}m1$ space group (refer to the ESI† of ref. 6 for the complete description of the crystal structure with atomic positions).

Fig. 3 shows X-ray diffractograms (XRD) of the initial phases and the final products of the Au-exchange process. Fig. 3(a) shows those of Ti_2AlC and Ti_2Au_2C. As can be seen, the Au-exchange reaction has made the lattice to expand along the *c* axis, shifting the 000*l* peaks of Ti_2AlC towards lower angles. Note that an 0002 peak for Ti_2AlC corresponds to an 0006 peak for Ti_2Au_2C with $P\bar{3}m1$ symmetry, as the *c* axis is three times larger. This corresponds to 33.5% of lattice swelling. Fig. 3(b) shows the X-ray diffractograms of Ti_3AlC_2 and $Ti_3Au_2C_2$, illustrating the same lattice swelling with the value of 26.7%. In both cases, the conversion from Ti_2AlC or Ti_3AlC_2 into Ti_2Au_2C or $Ti_3Au_2C_2$ is complete, as shown by the fact that the XRD peaks from the former phases are not present.

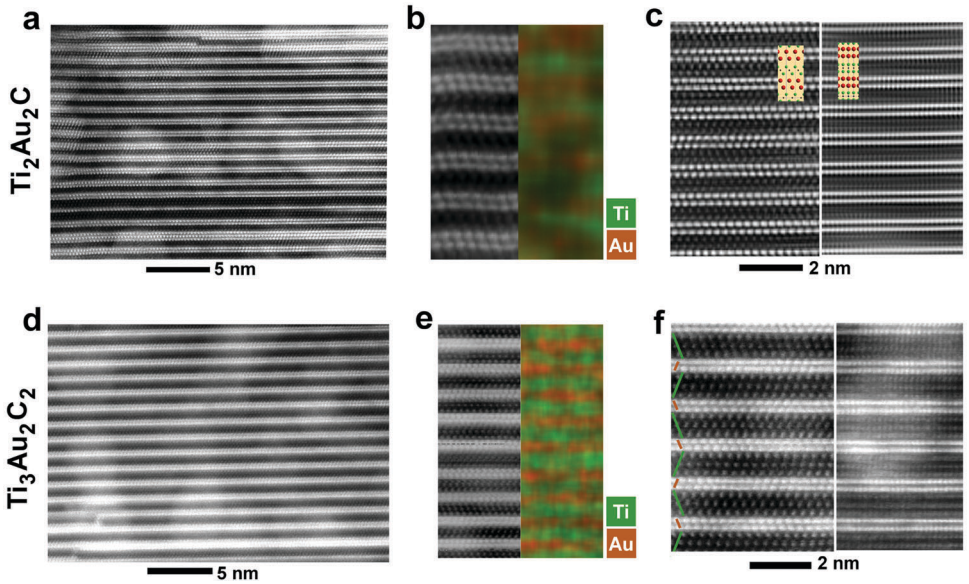

Fig. 2 (a) Low-resolution STEM of Ti_2Au_2C. (b) The corresponding high-resolution image together with the EDX mapping of Ti-Kα and Au-Kα. (c) The corresponding atomic positions from two different orientations with Ti, Au, and C atoms depicted in green, red, and black colors, respectively. (d), (e), and (f) the same as (a), (b), and (c), respectively for $Ti_3Au_2C_2$.

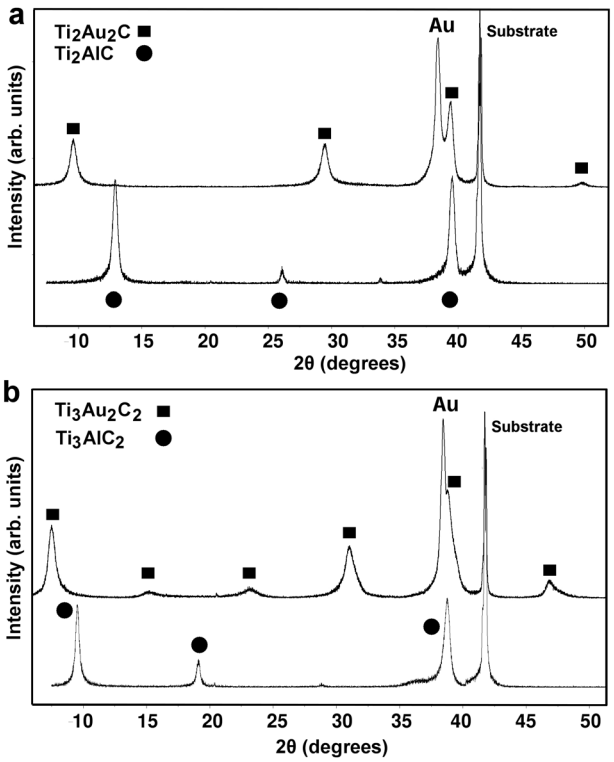

Fig. 3 (a) X-ray diffractograms of as-deposited Ti_2AlC and those of Ti_2Au_2C synthesized after the reaction process with Au. (b) Same as (a) for Ti_3AlC_2 and $Ti_3Au_2C_2$.

The substitution reaction in Ti_2AlC and Ti_3AlC_2, as well as in previously reported[6] Ti_3SiC_2 and Ti_3AuC_2, has kept the individual metal carbide layers intact, *i.e.*, it can also be described as a type of exchange–intercalation. This is in distinction to reports on reactions with other coinage metals (Cu and Ag), which indicate partial substitution of Cu and Ag for both M and A elements in MAX phases.[23,24] The present reaction requires high diffusivity for Au and Al to sustain the substitutional reaction in between the Ti_2C and Ti_3C_2 layers for the cases of Ti_2AlC and Ti_3AlC_2 hosts, respectively. The presence of a larger volume of Au is the driving force for Al atoms to out-diffuse from the $M_{n+1}AX_n$ phase. Based on the Al–Au phase diagram,[25] Al has about 14% of solubility in Au at 650 °C, the annealing temperature of our samples. At the same temperature and by increasing the Al content above the saturation level, the phase diagram contains either one-phase liquid- or two-phase liquid/solid regions, except for the very narrow region of solid $AuAl_2$ (≈1 at%), which can be neglected for our case due to its very little tolerance to changes in the stoichiometry. The presence of a liquid phase at 650 °C through the entire composition range of Al above its saturation level in Au–Al solid-solution is indicative of high atom diffusivity as well as the possibility for Al atoms to almost completely migrate to the surface of Au-capped samples. This is fully consistent with the previously reported case of Au exchange interaction within Ti_3SiC_2,[6] in that the Au–Si binary system is also comprised of either liquid or liquid/solid regions at the annealing temperature of the reaction.[25] This provides a general guideline for determining the thermodynamics of materials systems where this type of exchange reaction can be expected.

In conclusion, we reported synthesis of Ti_2Au_2C and $Ti_3Au_2C_2$ by a substitution reaction of Au in thin films of Ti_2AlC and Ti_3AlC_2. Exchange of Al-planes with Au-double layers resulted in 33.5% of lattice swelling for Ti_2AlC and 26.7% for Ti_3AlC_2. The crystal structures of Ti_2Au_2C and Ti_3Au2C_2 are in the $P\bar{3}m1$ space group rather than in the $P6_3/mmc$ space group of the regular MAX phases. These results and the described governing thermodynamics lead to a general guideline for identifying materials systems where this type of exchange reaction may occur.

The metal to be introduced should be inert towards the transition-metal carbide layers, and exhibit negative heat of mixing with the initial A element in a liquid phase or two-phase liquid/solid region at the annealing temperature. Therefore, the present demonstration of an Au-exchange reaction in Al-containing MAX phases is a strong indication of the generality of the process.

There are no conflicts of interest to declare.

We acknowledge support from the VINN Excellence Center in research and innovation on Functional Nanoscale Materials (FunMat) by the Swedish Governmental Agency for Innovation Systems and the Swedish Government Strategic Research Areas in Materials Science on Functional Materials at Linköping University (Faculty Grant SFO-Mat-LiU No. 2009 00971). P. E., J. L., M. D., and J. R. also acknowledge support from the Swedish Foundation for Strategic Research through the Future Research Leaders 5 program and the Synergy Grant FUNCASE, Functional Carbides and Advanced Surface Engineering. P. E. also acknowledges support from the European Research Council under the European Community's Seventh Framework Programme (FP/2007–2013)/ERC grant agreement no. 335383. We further acknowledge the Knut and Alice Wallenberg Foundation for a Scholar Grant (L. H.), Academy Fellow grants (J. R. and P. E.), and support to the Linköping Ultra Electron Microscopy Laboratory. The calculations were performed using resources provided by the Swedish National Infrastructure for Computing (SNIC) at the National Supercomputer Centre (NSC) and PDC.

References

1 M. S. Whittingham, *Prog. Solid State Chem.*, 1978, **12**, 41.
2 A. Van der Ven, J. Bhattacharya and A. A. Belak, *Acc. Chem. Res.*, 2013, **46**, 1216.
3 K. J. Koski, J. J. Cha, B. W. Reed, C. D. Wessells, D. Kong and Y. Cui, *J. Am. Chem. Soc.*, 2012, **134**, 7584.
4 J. Yao, K. J. Koski, W. Luo, J. J. Cha, L. Hu, D. Kong, V. K. Narasimhan, K. Huo and Y. Cui, *Nat. Commun.*, 2014, **5**, 5670.
5 J. P. Motter, K. J. Koski and Y. Cui, *Chem. Mater.*, 2014, **26**, 2313.
6 H. Fashandi, M. Dahlqvist, J. Lu, J. Palisaitis, S. I. Simak, I. A. Abrikosov, J. Rosen, L. Hultman, M. Andersson, A. Lloyd Spetz and P. Eklund, *Nat. Mater.*, 2017, **16**, 814.
7 M. W. Barsoum, *Prog. Solid State Chem.*, 2000, **28**, 201.
8 P. Eklund, M. Beckers, U. Jansson, H. Högberg and L. Hultman, *Thin Solid Films*, 2010, **518**, 1851.
9 Z. M. Sun, *Int. Mater. Rev.*, 2011, **56**, 143.
10 P. Eklund, J. Rosen and P. O. Å. Persson, *J. Phys. D: Appl. Phys.*, 2017, **50**, 113001.
11 M. Naguib, M. Kurtoglu, V. Presser, J. Lu, J. Niu, M. Heon, L. Hultman, Y. Gogotsi and M. W. Barsoum, *Adv. Mater.*, 2011, **23**, 4248.
12 M. Naguib, V. N. Mochalin, M. W. Barsoum and Y. Gogotsi, *Adv. Mater.*, 2014, **26**, 982.
13 B. Anasori, M. R. Lukatskaya and Y. Gogotsi, *Nat. Rev. Mater.*, 2017, **2**, 16098.
14 V. M. H. Ng, H. Huang, K. Zhou, P. S. Lee, W. Que, J. Z. Xu and L. B. Kong, *J. Mater. Chem. A*, 2017, **5**, 3039.
15 J. Zhou, X. Zha, F. Y. Chen, Q. Ye, P. Eklund, S. Du and Q. Huang, *Angew. Chem., Int. Ed.*, 2016, **55**, 5008.
16 L. Ding, Y. Wei, Y. Wang, H. Chen, J. Caro and H. Wang, *Angew. Chem., Int. Ed.*, 2017, **56**, 1825.
17 C. Hu, C.-C. Lai, Q. Tao, J. Lu, J. Halim, L. Sun, J. Zhang, J. Yang, B. Anasori, J. Wang, Y. Sakka, L. Hultman, P. Eklund, J. Rosen and M. W. Barsoum, *Chem. Commun.*, 2015, **51**, 6560.
18 C.-C. Lai, R. Meshkian, M. Dahlqvist, J. Lu, L.-Å. Näslund, O. Rivin, E. N. Caspi, O. Ozeri, L. Hultman, P. Eklund, M. W. Barsoum and J. Rosen, *Acta Mater.*, 2015, **99**, 157.
19 C.-C. Lai, H. Fashandi, J. Lu, J. Palisaitis, P. O. Å. Persson, L. Hultman, P. Eklund and J. Rosen, submitted for publication 2017 [included in C.-C. Lai, PhD thesis, ISBN 978-91-7685-526-3, in part available online at www.ep.liu.se].
20 J. Frodelius, J. Lu, J. Jensen, D. Paul, L. Hultman and P. Eklund, *J. Eur. Ceram. Soc.*, 2013, **33**, 375.
21 J. Emmerlich, D. Music, P. Eklund, O. Wilhelmsson, U. Jansson, J. M. Schneider, H. Högberg and L. Hultman, *Acta Mater.*, 2007, **55**, 1479.
22 Q. M. Wang, A. Flores Renteria, O. Schroeter, R. Mykhaylonka, C. Leyens, W. Garkas and M. to Baben, *Surf. Coat. Technol.*, 2010, **204**, 2343.
23 M. Nechiche, V. Gauthier-Brunet, V. Mauchamp, A. Joulain, T. Cabioc'h, X. Milhet, P. Chartier and S. Dubois, *J. Eur. Ceram. Soc.*, 2017, **37**, 459.
24 C. Lu, G. Wang, G. Yang, G. Fan, J. Zhang and X. Liu, *J. Am. Ceram. Soc.*, 2017, **100**, 732.
25 B. Predel, in *Ac–Au–Au–Zr*, ed. O. Madelung, Landolt-Börnstein – Group IV Physical Chemistry, Springer-Verlag, Berlin/Heidelberg, 1991, vol. A.